



A cryogenic chamber for scattering measurements

M.I. Lopes ^{a,*}, V. Chepel ^a, A. Kuchenkova ^{a,1}, O.D. Gonçalves ^b, H. Schechter ^b

^a LIP-Coimbra, Departamento de Física, Universidade de Coimbra, 3000 Coimbra, Portugal

^b Inst. Física, Universidade Federal do Rio de Janeiro, P.O. Box 68528, 21945-970 Rio de Janeiro, Brazil

Received 28 July 1998; received in revised form 13 December 1998

Abstract

We have constructed a cryogenic chamber to measure scattering cross sections of photons in liquids of low-boiling point. The chamber was tested with liquid xenon using a ¹³⁷Cs radioactive source emitting 662 keV photons. The spectra obtained are presented and analyzed, attesting the good performance of the chamber for the desired purposes. © 1999 Elsevier Science B.V. All rights reserved.

PACS: 13.60.Fz; 07.05.Fb; 07.85.-m; 07.20.Mc

Keywords: Rayleigh scattering; Compton scattering; Liquid xenon

1. Introduction

Gamma-rays scattering plays a very important role in basic and applied sciences. The elastic (Rayleigh) and inelastic (Compton) scattering of photons have been extensively studied, both experimentally and theoretically, for the energy range from 10 to 1000 keV and for large momentum transfers (typically, $x > 2 \text{ \AA}^{-1}$, where $x = 1/\lambda \sin(\theta/2)$ with $\lambda(\text{\AA}) = 12.4/E$ (keV), E being the photon energy and θ the scattering angle). The differential cross sections have been measured

mostly in solid samples with uncertainties lower than 5% [1]. Calculations for those high-momentum transfers are usually performed in the free atom approximation [1]. Extensive tabulations are available based either on form factor approximation [2] or second order perturbation theory [1]. A general agreement within 10% has been achieved.

In the case of photon scattering involving small momentum transfer (typically corresponding to $x < 2 \text{ \AA}^{-1}$) in complex environments like crystals, polycrystalline aggregates and liquids, the structure of the medium leads to interference effects [3]. For liquids, few experimental and theoretical data are available [3–5]. In many cases the scattering process can still be described as being due to free atoms, depending on factors like temperature, atomic number or preparation of the sample. Hence, each particular case has to be investigated before using the free atom approximation [3].

* Corresponding author. Tel.: +35139410657; fax: +35139822358; e-mail: isabel@lipc.fis.uc.pt

¹ On leave from Institute of Theoretical and Experimental Physics, Moscow, Russian Federation.

Such complex structures are specially important in appliances involving X- and γ -rays. New detectors are being developed using new materials and therefore an accurate knowledge of the differential scattering cross sections in those media is fundamental. Among the liquids, xenon has an additional reason to be investigated. Indeed, a new detector based on liquid xenon is being developed for positron emission tomography (PET) [6], and the details of its operation and optimization require the knowledge of the differential cross section for coherent and incoherent scattering [7].

Here we report on the construction and performance of a cryogenic chamber for measurement of photon scattering cross sections in liquids of low-boiling point. The tests were done with liquid xenon and 662 γ -rays.

2. Chamber

In view of its application, the chamber was designed to fulfill the following requirements: (1) the container walls must be as thin as possible and made of low- Z materials, so as to minimize the scattering background; (2) the geometry should be compact in the scattering plane, in order to avoid large uncertainty in the determination of the effective scattering angle; (3) the linear dimensions of the sample in the scattering plane should be smaller or comparable to the mean free path of the photons in the sample, to minimize multiple scattering in the medium; (4) the whole liquid sample has to be irradiated to allow the calculation of the number of atoms participating in the scattering, and so the absolute differential cross section; (5) the cell in which the gas is liquefied should be replaceable, so that different samples and photon energies could be used.

A schematic drawing of the chamber is shown in Fig. 1. It includes an aluminum inner cell ($\text{Ø}20 \times 50 \text{ mm}^3$ inner dimensions, 1 mm wall thickness), where the liquid sample is condensed, which was dimensioned in view of the tests with liquid xenon and 662 keV γ -rays. Hence, its inner diameter is smaller than the mean free path of those photons in that medium ($\approx 4 \text{ cm}$).

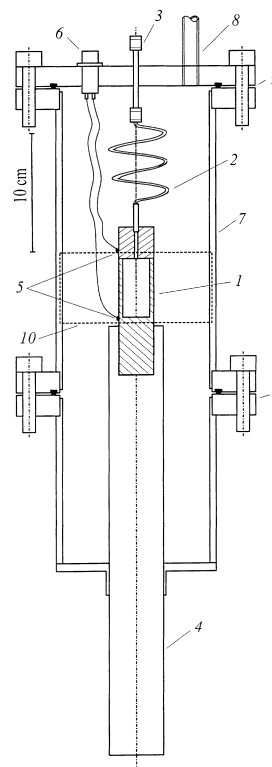


Fig. 1. Drawing of the chamber: (1) inner cell; (2) helical tube; (3) gas inlet; (4) copper cold finger; (5) thermoresistors; (6) multipin feedthrough; (7) outer vessel; (8) connection to vacuum pump; (9) CF flanges; (10) carbon fiber window.

The cell is placed inside a stainless steel vessel (70 mm outer diameter, 2 mm wall thickness) closed on the top with a CF² flange sealed with a copper ring. To facilitate the assembly, the body of the chamber is made of two cylindrical parts connected by another CF flange. A thick copper rod of $\text{Ø}30 \text{ mm}$, crossing the bottom of the outer vessel and welded to it, has the inner cell threaded into its upper end. This rod functions as a cold finger which, when immersed in a cold bath, allows the inner cell to be cooled down. To decrease the heat exchange between the liquid sample and the surroundings, a vacuum jacket is created around the cell by pumping the outer vessel with a vacuum

² Conflat flange, trademark of Varian, Palo Alto, California, USA.

pump connected to the upper flange (see Fig. 1). The uniformity of temperature along the inner cell is achieved by means of a copper piece (not shown in Fig. 1) connecting the extremities of the cell. The temperature is monitored by two platinum thermoresistors³ glued on the top and the bottom of the inner cell. The entrance of gas, as well as the evacuation of the inner cell, is made through a long stainless steel tube ($\varnothing 3$ mm) wound in a helical form and connected by a Swagelok⁴ coupling to the top flange of the outer vessel. This helix is flexible enough to allow the assembly of the whole chamber. To minimize scattering in the walls of the outer vessel that would disturb the measurements for which the chamber is designed, the outer vessel has a thin lateral window of carbon fiber (low-*Z* material) with a thickness of about 0.5 mm, covering an angle of 270° .

It is worthwhile to notice two characteristics of this chamber that extend its applicability: (i) it can be used with different inner cells, a feature which is very useful to perform scattering measurements with radiation of different energies that require samples of different sizes; (ii) the temperature in the inner cell can be varied by using a suitable cooling bath, thus allowing the use of the chamber for carrying out measurements at different temperatures and with different cryogenic liquids.

3. Chamber tests

Before assembling the chamber, the inner cell was tested for leaks with nitrogen gas at pressures up to 50 bar at room temperature and at -196°C , and in vacuum (also at room and low temperatures) with a helium leak tester.

The vacuum and gas supply system is depicted in Fig. 2. The thermal behavior of the chamber was tested with the cell filled with liquid xenon, which can exist in the liquid phase between -112°C and $+16^\circ\text{C}$ (triple and critical points, respectively), the pressure of gas in contact with the liquid varying between 0.8 and 58 bar, respec-

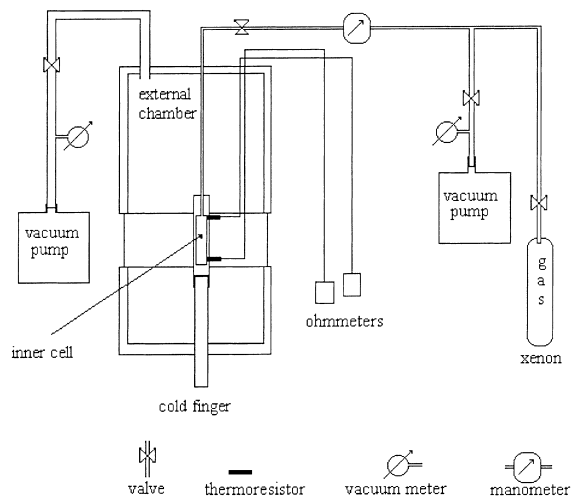


Fig. 2. Schematic drawing of the vacuum and gas supply system.

tively. Within this range of temperatures the liquid density varies between 3.1 and 1.1 g/cm^3 . In order to achieve the required low temperature, a bath of ethyl alcohol cooled with liquid nitrogen was used whose temperature is monitored by a thermoresistor. When the alcohol gets partially frozen, its temperature stabilizes around -115°C (the exact value depends on the alcohol grade) lowering the cell temperature down to -95°C .

Before the cooling procedure is started, the outer vessel and the inner cell are pumped down to 10^{-3} mbar. Then, the cold finger of the chamber is immersed into the cooling bath, while the outer vessel continues to be pumped. When the temperature of the cell reaches the required value, the valves connecting the xenon container with the inner cell are opened (see Fig. 2) and the xenon gas flows into the cell where it condenses. The level of liquid xenon inside the cell is monitored by measuring the attenuation of a highly collimated beam of 60 keV photons from an ^{241}Am source that can be moved vertically (see Fig. 4). This method is checked by calculating the amount of gas condensed in the chamber from the knowledge of the variation of the pressure in the gas bottle during the filling procedure.

When the measurements are finished, the gas is collected back into the bottle by immersing this

³ Pt100 sensors from Minco EC AG, Sirmach, Switzerland.

⁴ Swagelok Co., Solon, OH44139, US.

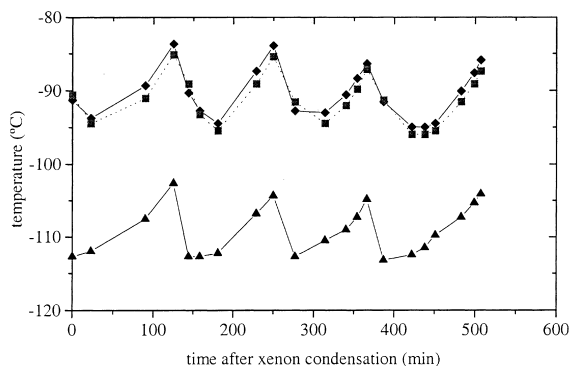


Fig. 3. Typical variation of temperature in the cell during data acquisition, as measured in the bath (\blacktriangle) and at the bottom (\blacklozenge) and top (\blacksquare) of the cell.

bottle into a dewar with liquid nitrogen and removing the bath to let the cell warm up.

The variation of temperature of the cell and the bath after condensing the xenon is shown in Fig. 3 for a period of 8 h which was a typical acquisition time. Due to the heat exchange with the environment, the bath warms up slowly and so does the inner cell. To compensate for this effect, liquid nitrogen was added to the bath periodically, cooling it down. Hence, the temperature fluctuates as shown in Fig. 3, resulting in insignificant variations of the xenon density ($\leq 1\%$) which are sufficiently small to perform the scattering measurements. The fact that the top of the cell is usually slightly cooler than its bottom (except for the moments when liquid nitrogen is added) indicates that the bath warming is the determinant factor responsible for the rising of the cell temperature. Hence, the temperature fluctuations can be easily reduced by improving the thermal insulation of the bath container (the one presently used, made of styrofoam, will be replaced by a conventional dewar with obvious advantages) or by adding liquid nitrogen more frequently.

The temperature gradient between the bottom and the top of the chamber did not exceed 2° .

4. Experimental setup

The experimental arrangement to be used in the scattering cross section measurements is repre-

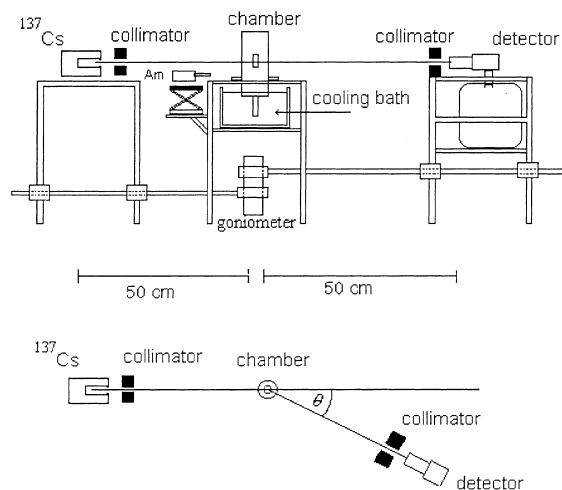


Fig. 4. Experimental setup used for the scattering differential cross section measurements.

sented in Fig. 4. A 200 mCi (7.4 GBq) ^{137}Cs (662 keV γ -rays) source with an active diameter of 5 mm was used. A collimator constrains the γ -beam incident on the sample within a solid angle $\Omega_b = 4 \times 10^{-3}$ sr, sufficient to guarantee that the whole liquid sample in the cell is inside the radiation beam and the sample is uniformly irradiated. There is the possibility that a small amount of liquid present in the thin tube above the cell (less than 1% of the cell content) is also irradiated, but its contribution to the total amount of scattered photons is much smaller than the statistical error in a typical scattering experiment which varies from 3% to 30% depending on the scattering angle, as described in Section 5.

At the γ -ray energy used (662 keV), both Compton and Rayleigh scattering can occur [1]. The radiation scattered by the sample was detected with a $\varnothing 32$ mm high-pure Ge-detector, with active layer of 13 mm and 0.254 mm Be-window, whose energy resolution is about 0.1% for 662 keV photons. The detector can be rotated in the horizontal plane and placed at different angles θ , with an accuracy of about $\pm 0.1^\circ$. A 1 cm wide and 2.65 cm high collimator is placed in front of the detector, subtending a solid angle $\Omega_d = 3.6 \times 10^{-3}$ sr, which is just large enough to view the whole sample.

To analyze the detector signals, a conventional read-out and data acquisition system was used

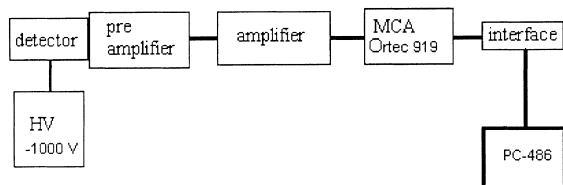


Fig. 5. Read-out and data acquisition system.

(Fig. 5). After amplification, the detector signal is processed in a multichannel analyzer where the energy spectrum of the scattered radiation is recorded.

5. Assessment of the chamber performance

To assess the chamber performance in scattering experiments, the photon spectra were measured at different scattering angles ranging from 3° to 25° . At each angle, the photons that reach the detector after single elastic or single inelastic scattering produce two peaks (which overlap at small angles), easily distinguishable from the nearly uniform low-energy background due to multiple scattering. In Figs. 6–9, spectra taken at 3° , 5° , 16° and 25° are shown. Each figure presents the whole spectra (A) and the region containing the Compton and Rayleigh peaks (B). For 16° (Fig. 8) we have also included a third graph (C) showing only the Rayleigh peak. In each case, three spectra are represented: the first (labeled F) was obtained with the chamber filled with liquid Xe and the second (labeled E) with the evacuated chamber. The third spectrum (labeled S), obtained by subtracting the second spectrum from the first after acquisition time normalization, is related only to the scattering by the liquid Xe.

From the figures, one can see that:

1. The elastic scattering peak is very clear at 5° and 16° and well separated from the peak due to Compton scattering.
2. As it can be observed in the spectrum taken at 3° (Fig. 6), the peaks corresponding to elastic and Compton scattering overlap at angles below 5° , due to the decrease of the Compton shift with decreasing scattering angle, and cannot be resolved. However, since the Compton differ-

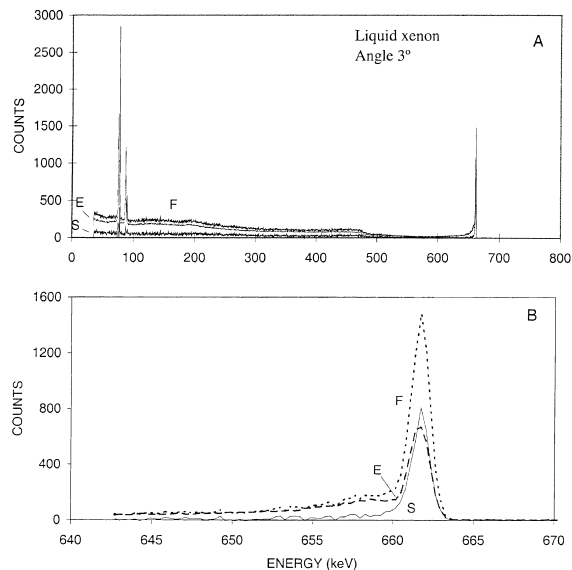


Fig. 6. Scattering spectra for liquid xenon obtained at 3° : (A) whole spectra; (B) Compton and Rayleigh energy region (F – full chamber; E – empty chamber; S = F – E).

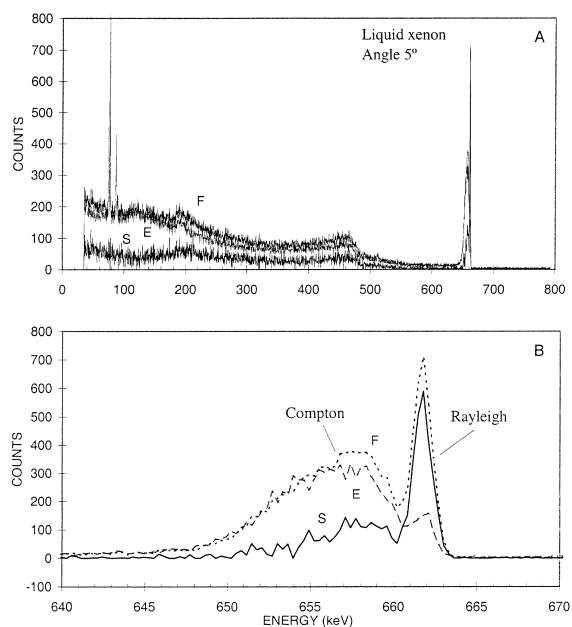


Fig. 7. Scattering spectra for liquid xenon obtained at 5° : (A) whole spectra; (B) Compton and Rayleigh energy region (F – full chamber; E – empty chamber; S = F – E).

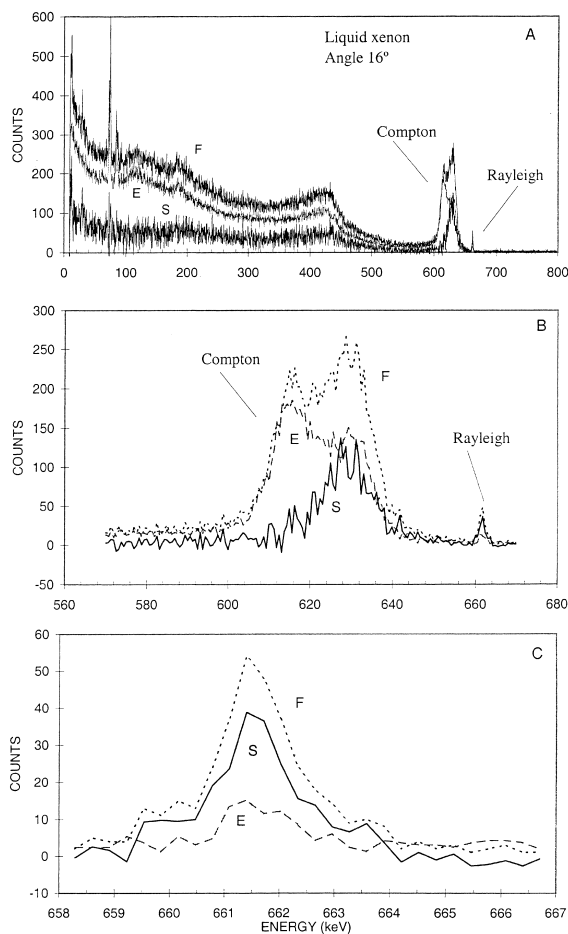


Fig. 8. Scattering spectra for liquid xenon obtained at 16°: (A) whole spectra; (B) Compton peak; (C) Rayleigh peak region (F – full chamber; E – empty chamber; S = F – E).

tial cross section is much smaller than the Rayleigh differential cross section, the latter can still be estimated regarding the inelastic contribution as an uncertainty, with the subsequent decrease of the precision in the determination of the elastic cross section.

- Due to the sharp decrease of the differential elastic cross-section with scattering angle, the peak corresponding to elastic scattering at large angles (see spectrum at 25° in Fig. 9) is very small, remaining almost unresolved even for a long acquisition time (≈ 15 h).
- The Compton spectra (measured with the chamber full and empty) present a complex peak (see

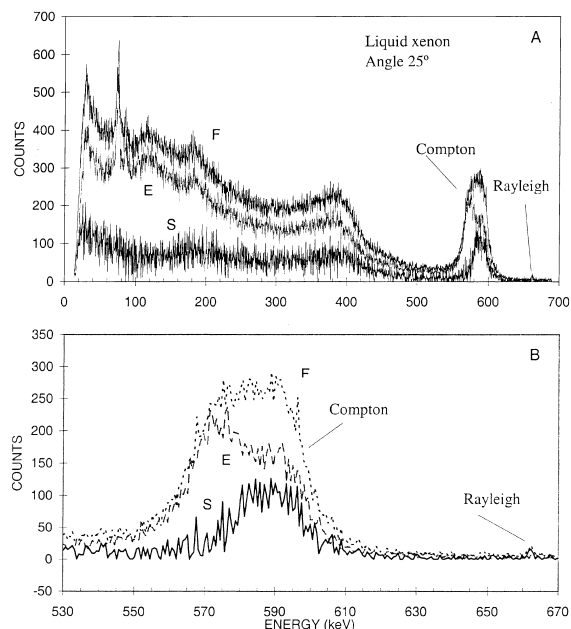


Fig. 9. Scattering spectra for liquid xenon obtained at 25°. (A) whole spectra; (B) Compton and Rayleigh energy region (F – full chamber; E – empty chamber; S = F – E).

Fig. 8 and Fig. 9), due to the different angles related to the scattering in the four walls, two of the inner chamber (aluminum) and two of the outer chamber window (carbon fiber). Nevertheless, the subtraction spectrum has a single peak, thus allowing the Compton differential cross sections to be computed.

6. Conclusion

The chamber built for performing measurements of γ -rays scattering in liquids of low-boiling point was successfully tested with liquid xenon. Indeed, the chamber was operated at the temperature of $(-86 \pm 6)^\circ\text{C}$ for the long periods of time required for the data taking. The fluctuations in the temperature can be further reduced by using a conventional dewar as the container for the cooling bath.

For 662 keV γ -rays, the setup is suitable for measurements of elastic scattering cross-sections at angles larger than 5° and above 10° approximately

for the case of inelastic scattering. However, the measurements become difficult to perform at large angles, i.e. $\geq 25^\circ$, due to the very long counting time required. Since there is more interest in studying elastic scattering at low angles for which the cross section is larger and can deviate from the values expected on the basis of the free atom approximation, the camera fulfills the desired performance.

For future applications scattering measurements with γ -rays of lower energies can also be carried out, since the chamber design allows the use of different inner cells.

Acknowledgements

We would like to thank the Agencies ICCTI (Instituto de Cooperação Científica e Tecnológica

Internacional) from Portugal and CAPES (Coordenação de Aperfeiçoamento de Pessoal de Nível Superior) from Brasil for supporting this project.

References

- [1] P. Kane, L. Kissel, R. Pratt, S. Roy, Phys. Rep. 140 (1986) 75.
- [2] J.H. Hubell, W.J. Veigle, E.A. Briggs, R.T. Brown, D.T. Cromer, R.J. Howerton, J. Phys. Chem. Ref. Data 4 (1975) 471.
- [3] O.D. Gonçalves, W.M.S. Santos, J. Eichler, A.M. Borges, Phys. Rev. A 49 (1994) 4405.
- [4] L.R.M. Morin, J. Phys. Chem. Ref. Data 11 (1982) 1091.
- [5] D.A. Bradley, D. Dance, S.H. Evans, C.H. Jones, Nucl. Instr. and Meth. A 280 (1989) 380.
- [6] V. Chepel, M.I. Lopes, R. Ferreira Marques, A.J.P.L. Policarpo, Nucl. Instr. and Meth. A 392 (1997) 427.
- [7] M.I. Lopes, V. Chepel, J. Carvalho, R. Ferreira Marques, A.J.P.L. Policarpo, IEEE Trans. Nucl. Sci. 42 (1995) 2298.